Journal of Magnetics 26(1), 67-70 (2021)
ISSN (Print) 1226-1750
ISSN (Online) 2233-6656
https://doi.org/10.4283/JMAG.2021.26.1.067

Effects of Annealing Temperature on Amorphous $Co_{67}Fe_3Cr_3B_{12}Si_{15}$ Alloys for Flux-gate Magnetometers

Deok Young Lee[1]*, Sin Hyuk Yim[1], and Derac Son[2]*

[1]*Agency for Defense Development, Yuseong P.O. Box 35, Daejeon, Republic of Korea*
[2]*Sensorpia, Yuseong-daero 1596-64, Daejeon 34054, Republic of Korea*

(Received 4 January 2021, Received in final form 27 March 2021, Accepted 29 March 2021)

The magnetic properties of amorphous alloy $Co_{67}Fe_3Cr_3B_{12}Si_{15}$ samples, which were produced by the melt-spinning method and annealed at various temperatures, are analyzed. We found the best annealing temperature for $Co_{67}Fe_3Cr_3B_{12}Si_{15}$ was 350 °C for 1 hour at 30 mTorr. We also produced a flux-gate magnetometer with the annealed samples with the best magnetic properties. The flux-gate sensor shows a noise level of 2.4 pT$\sqrt{Hz}$ at 1 Hz, and 0.1 nT_{p-p} in the frequency domain with 1 Hz bandwidth.

Keywords : amorphous, annealing, flux-gate, magnetometer

1. Introduction

Flux-gate type magnetometers have been used as low-magnetic field measuring sensors since they were first developed before World War II [1] and have been used since the 1960s to control the attitude of rockets and satellites [2], to measure magnetic fields in space [3] and changes in geomagnetic fields [4]. Their application range today is very diverse, and they are used for non-destructive testing [5, 6] and detecting and imaging underground objects to detect explosives [7]. The flux-gate magnetometer has many advantages for measuring slowly fluctuating magnetic fields, especially in areas where the low-magnetic field measuring technology requires long-term stability. To exploit these advantages and improve the resolution of flux-gate sensors, and develop sensors with lower power consumption, an amorphous soft magnetic alloy ribbon with excellent magnetic properties should be used [8].

One of the most important parameters that characterize the performance of the magnetic sensor is magnetic noise. Previous studies so far have shown that the noise level of this sensor depends primarily on the quality of the amorphous soft magnetic alloy ribbon used in the core of the flux-gate magnetometer. The core material for sensor performance to reduce the noise of the sensor should have the following properties [9]: close to zero magnetostriction, low values of saturation magnetization, low values of coercive force, and maximal initial permeability. Using the materials that meet the above conditions can result in less energy loss of hysteresis and higher magnetometer sensitivity. As a result, the materials have a hysteresis curve with low Barkhausen noise levels. The Barkhausen noise in a flux-gate magnetometer is one of the limiting factors for the performance [10, 11].

2. Materials and Sample Preparation

Co-based amorphous soft magnetic alloys are suitable for flux-gate application because the alloys have low saturation magnetization, almost zero magnetostriction, and high permeability, which reduces power consumption in magnetometers [12]. Also, the properties of Co-based amorphous soft magnetic alloys can be tuned by annealing. Increasing the temperature of annealing creates the energy needed to remove impurities in the structure of materials, and there are structural improvements that help the domain wall movement and rotation, creating a hysteresis loop with lower coercivity. If annealing is carried out above a certain temperature for each alloy, the noise level of the sensor begins to increase again due to the increment of magnetic domain size. This result is due to the start of partial crystallization, which results in poor AC characteristics [13]. In our experiments, we measured

*Co-corresponding author: Tel: +82-42-607-6118
e-mail: dleeao@add.re.kr
Tel: +82-42-933-0877, e-mail: sensorpia@ sensorpia.co.kr

the magnetic properties of $Co_{67}Fe_3Cr_3B_{12}Si_{15}$ alloys as a function of the temperature of the annealing process to find the optimal annealing temperature of the material for the sensor. We changed some composition of the well-known Co-based amorphous alloy (Metglas 2714A, $Co_{66}Fe_4Ni_1B_{14}Si_{15}$) into Cr. With a previous study showing that the addition of Cr improves glass-forming ability and also improves the corrosion resistance of the alloy [14, 15], we expected the composition of our sample to be suitable for defense technology.

Amorphous alloys are generally manufactured using a melt-spinning method that prevents the material from being crystallized. The molten material is sprayed onto a cooled copper wheel rotating at a sufficiently high angular speed. In this study, an amorphous alloy with the composition $Co_{67}Fe_3Cr_3B_{12}Si_{15}$ was prepared by melt-spinning. The alloy was manufactured in the form of ribbons, typically 18 μm thick, and slit as 3 mm wide. The samples were isothermally annealed at various temperatures in a vacuum oven for 1 hour. After annealing, the samples were slowly cooled to room temperature.

3. Results and Discussion

We found from previous studies that for Metglas 2714A, optimal annealing can be achieved at approximately 300-350 °C [16, 17]. In our composition $Co_{67}Fe_3Cr_3B_{12}Si_{15}$, the addition of Cr results in an annealing effect at lower temperatures because the addition of Cr decreases the Curie temperature of the amorphous alloy and also modifies the alloy crystallization temperature [18, 19]. From this knowledge, we annealed the $Co_{67}Fe_3Cr_3B_{12}Si_{15}$ sample from 200 °C to 400 °C. There was no significant effect of annealing below 300 °C, *e.g.*, there was no significant change in the hysteresis curve, and we found out that crystallization of the sample began at 400 °C. Therefore, we would like to show the data of as-quenched samples and annealed samples above 300 °C and below 400 °C. Figure 1 shows the measured DC B-H hysteresis loops of the $Co_{67}Fe_3Cr_3B_{12}Si_{15}$ samples in the as-quenched and after annealing at various temperature conditions, respectively. We measured the DC B-H loop according to the standard IEC 60404-4 with a yoke-type permeameter and DC hysteresis loop tracer [20]. The $Co_{67}Fe_3Cr_3B_{12}Si_{15}$ ribbons exhibited 0.33 T of saturation magnetization. The as-quenched sample had a coercive field of 4.9 A/m. The annealed samples had a lower DC coercive field, of 1.43 A/m, 1.35 A/m at the annealing temperatures of 350 °C, 375 °C, respectively. As with the results of the experiment, it is caused by nano-crystallization that lowers the coercive field by annealing [21, 22]. It is well known that

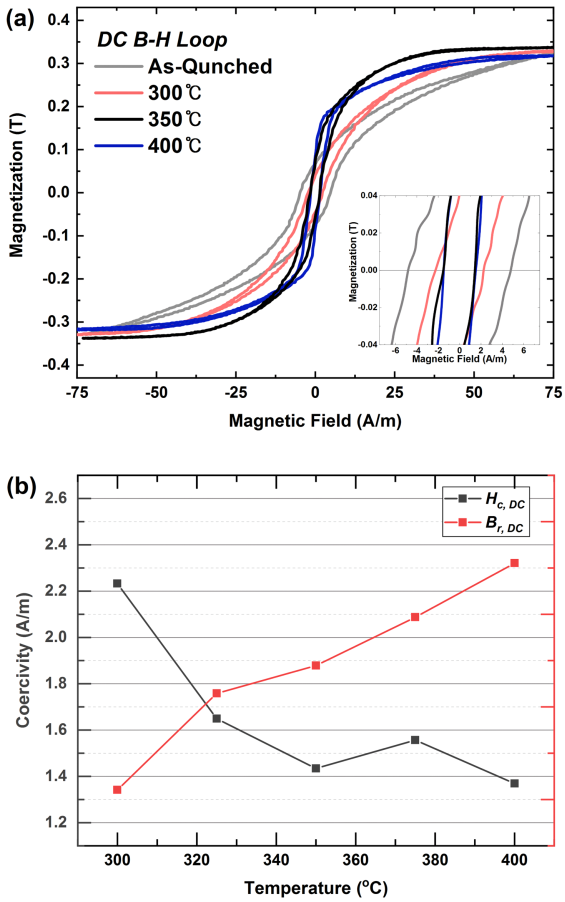

Fig. 1. (Color online) (a) Several selected DC B-H hysteresis loops for as-quenched and annealed samples of amorphous $Co_{67}Fe_3Cr_3B_{12}Si_{15}$ alloys. The inset shows an enlarged view. (b) Changes of coercive field ($H_{c,DC}$) and residual field ($B_{r,DC}$) depends on the annealing temperature.

the control of the microstructure of the nano-crystallized amorphous ribbons depends heavily on the composition of the amorphous alloys, the annealing temperature, and the annealing time [23-25]. As a result of measuring DC B-H hysteresis loops, in the case of the $Co_{67}Fe_3Cr_3B_{12}Si_{15}$ samples, we have found that if annealing is carried out for 1 hour, the annealing temperature between 300 °C and 400 °C is most suitable.

Figure 2 shows measurements of the AC B-H hysteresis loops of the annealed $Co_{67}Fe_3Cr_3B_{12}Si_{15}$ samples in 10 kHz of AC frequency. We proceeded with the measurement for the selected samples which are annealed at temperatures of 300 °C, 325 °C, 350 °C, 375 °C, 400 °C. We measured the AC B-H loops with a single sheet type AC hysteresis loop tracer with a ferrite yoke.

The $Co_{67}Fe_3Cr_3B_{12}Si_{15}$ ribbons also exhibited about 0.33 T of saturation magnetization. However, the coercive field of the sample prepared at an annealing temperature

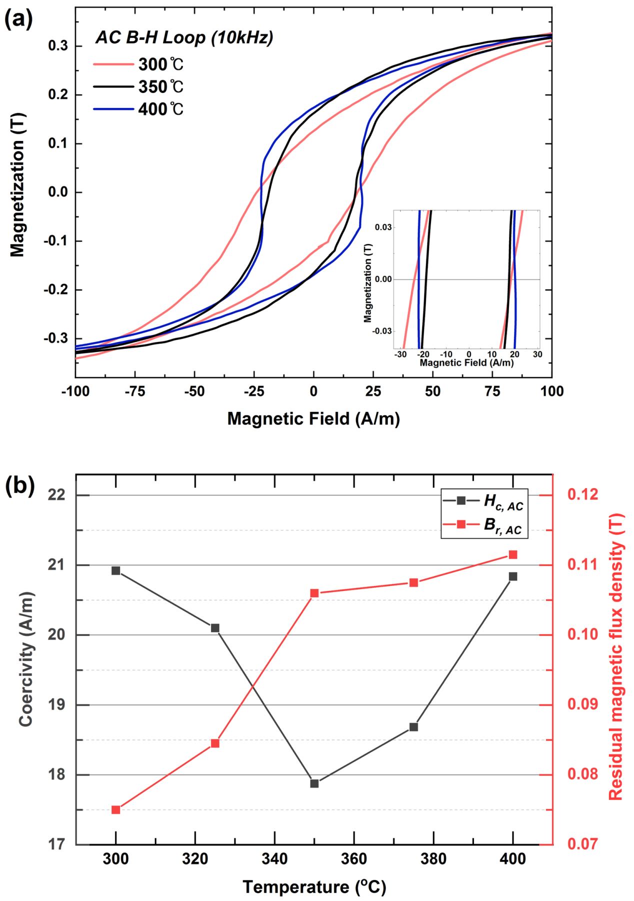

Fig. 2. (Color online) (a) Several selected 10 kHz AC B-H hysteresis loops for annealed samples of amorphous $Co_{67}Fe_3Cr_3B_{12}Si_{15}$ alloys. The inset shows an enlarged view. (b) Changes of coercive field ($H_{c,AC}$) and residual field ($B_{r,AC}$) depends on the annealing temperature.

of 350 °C had the lowest value of 18.2 A/m in the 10 kHz AC measurement. An annealing temperature higher or lower than 350 °C increased the coercive field.

This result was interpreted to be a result of the size of the magnetic domains in the annealed sample. An annealing temperature exceeding 350 °C increases the crystallization of the sample. As the annealing temperature increases, the size of the magnetic domains becomes larger. Using a random anisotropy model in amorphous materials [26], there is a relation between coercive field and domain size as $H_c \propto D^6$ by Herzer [27].

When the annealing temperature of the sample increased, the DC coercive field of the sample seems to be decreased. However, samples with larger magnetic domains need more energy to move during magnetization. Accordingly, the 10 kHz AC coercive field deteriorated as the temperature was increased. The results of AC characterizations indicated that the annealed sample had a higher magnetic

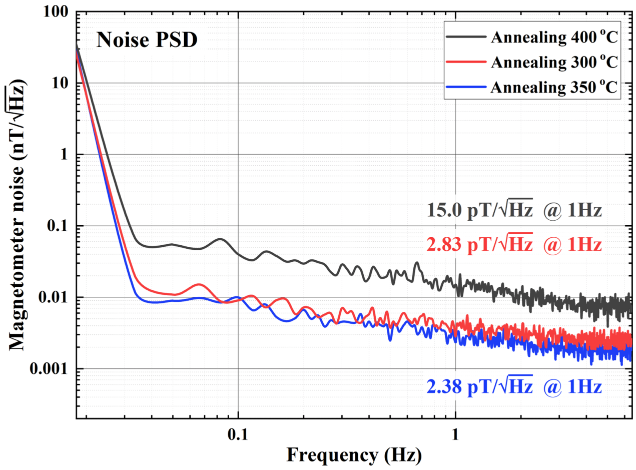

Fig. 3. (Color online) The noise power spectral density(PSD) of the flux-gate magnetometer manufactured from annealed $Co_{67}Fe_3Cr_3B_{12}Si_{15}$ at temperatures of 300 °C, 350 °C, 400 °C.

Barkhausen noise, which will increase the noise of the sensor, with increasing temperatures above 350 °C.

We made a flux-gate magnetometer using the annealed samples as a magnetic core to investigate the characteristics of the samples in sensors. We chose a closed sensor race-track type with low noise because its demagnetization factor is low [9, 28]. The primary coil that magnetizes the core was wound with a 0.2 mm diameter enamel copper wire. The secondary coil for measuring magnetic flux changes and compensating the measured magnetic field was wound 600 times with 0.12 mm diameter enamel copper wire on a round bobbin with a diameter of 8 mm and a length of 45 mm. The signal processing and the measurement of noise characteristics,

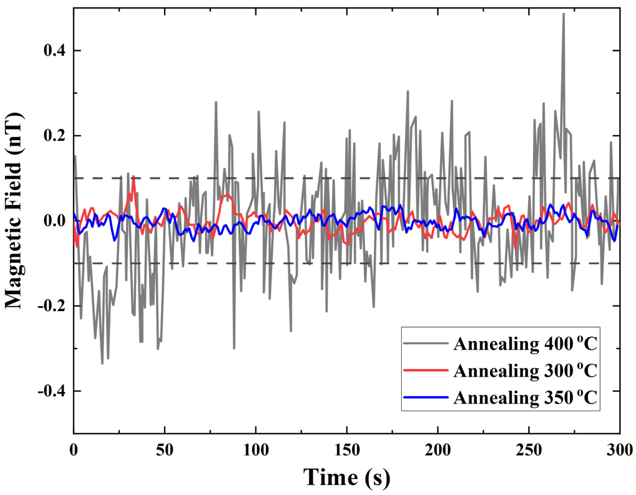

Fig. 4. (Color online) Time plot of the noise of the flux-gate magnetometer manufactured from annealed $Co_{67}Fe_3Cr_3B_{12}Si_{15}$ at temperatures of 300 °C, 350 °C, 400 °C.

and the stability of the long-term zero points of the sensor were performed following the methods reported by D. Son [16]. The modulated magnetic field signal was amplified using an operational amplifier, which magnetized the core material. A demodulator and low-pass filter were used to pass only the second harmonic signals from the secondary coil to select them from the magnetic field to be measured. The output of the low-pass filters was entered into the secondary coil after going through the feed-back amplifier, making the actual magnetic field received by the core material a zero magnetic field. Since the voltage applied to the secondary coil is proportional to the magnetic field to be measured, this voltage, electromotive force, was used to convert the digital signal, using a 24-bit analog to digital converter.

The noise power spectral density and time plot of the noise of the flux-gate magnetometers with annealed $Co_{67}Fe_3Cr_3B_{12}Si_{15}$ as the sensor core are shown in Figure 3 and Figure 4. Our flux-gate magnetometers achieved $2.8\ pT/\sqrt{Hz}$, $2.4\ pT/\sqrt{Hz}$, $15.0\ pT/\sqrt{Hz}$ at 1 Hz of noise level with the samples annealed at the temperatures of 300 °C, 350 °C, 400 °C, respectively. The optimal result obtained from this experiment is approximately twice as good as the result of a previous study($5\ pT/\sqrt{Hz}$ at 1 Hz) that we obtained using the Metglas 2714A core [16].

The time plot indicates the time-domain noise level under 1 Hz bandwidth for 300 seconds inside of magnetic shield chamber with 100 dB shielding factor [17]. While the 350 °C annealed sample was stable within 0.1 nT peak-to-peak, the 400 °C annealed sample was higher than 1nT peak-to-peak.

4. Conclusion

In our experiments, we annealed the Co-based amorphous soft magnetic alloy, $Co_{67}Fe_3Cr_3B_{12}Si_{15}$, at various temperatures, and measured their magnetic properties and characteristics in a flux-gate magnetometer, in an effort to develop a flux-gate magnetometer with excellent resolution, low consumption power, and excellent long-term stability. We determined that $Co_{67}Fe_3Cr_3B_{12}Si_{15}$ ribbons annealed at a temperature of 350 °C could be used as long-term highly stable core materials for flux-gate magnetometers with a low noise level. Also, we found that the $Co_{67}Fe_3Cr_3B_{12}Si_{15}$ ribbons have potential uses in various high-frequency applications.

Acknowledgments

$Co_{67}Fe_3Cr_3B_{12}Si_{15}$ ribbons were prepared by a melt-spinning method in Amo-Greentech Co., Rep. of Korea. This research was supported by the Agency for Defense Development (ADD), Rep. of Korea.

References

[1] D. I. Gordon, IEEE Trans. Magn. **8**, 8 (1972).
[2] M. H. Acuna, Rev. Sci. Instrum. **73**, 3717 (2002)
[3] A. W. Yau and H. G. James, Space Sci. Rev. **189**, 3 (2015).
[4] A. Hemshorn, H. U. Auster, and M. Fredow, Meas. Sci. Technol. **20** (2009) 027004.
[5] Z. Zhou, et al., IEEE Sens. J. **20**, 7661 (2020).
[6] D. Son, et al., J. Magn. **14**, 97 (2009).
[7] S. Gürkan et al., Appl. Sci. **9**, 5415 (2019).
[8] P. Ripka, Sensors and Actuators A **106**, 8 (2003).
[9] V. Korepanov and A. Marusenkov, Surv. Geophys. **33**, 1059 (2012).
[10] J. L. M. J. van Bree, et al., Appl. Sci. Res. **29**, 59 (1974).
[11] G. P. Farrell and E. W. Hill, IEEE Trans. Man. **31**, 4050 (1995).
[12] F. Fiorillo, et al., "Soft Magnetic Materials", Wiley Encyclopedia of Electrical and Electronics Engineering, (2016).
[13] J. S. Yang, D. Son, Y. Cho, and K. S. Ryu, J. Magn. **2**, 130 (1997).
[14] J. Han, J. Hong, S. Kwon, and H. Choi-Yim, Metals **11**, 304 (2021).
[15] T. Masumoto and K. Hashimoto, J. Phys. Colloq. **41**, C8-894-C8-900 (1980).
[16] D. Son, J. Korean. Magn. Soc. **22**, 45 (2012). [in Korean]
[17] E. Kim and Derac Son, J. Korean. Magn. Soc. **24**, 123 (2014). [in Korean]
[18] P. Marin, M. Lopez, and A. Hernando, J. Appl. Phys. **92**, 374 (2002).
[19] R. C. O'Handley, Solid State Commun. **38**, 703 (1981).
[20] "Methods of measurement of DC magnetic properties of magnetically soft materials", International Standard, IEC 60404-4:1995+AMD1:2000+AMD2:2008 CSV.
[21] Y. Yoshizawa, S. Oguma, and K. Yamauchi, J. Appl. Phys. **64** (1988) 6044.
[22] G. Herzer, IEEE Trans. Magn. **26**, 1397 (1990).
[23] K. Suzuki, et al., Mater. Trans. **31**, (1990).
[24] G. C. Hadjipanayis, J. Magn. Magn. Mater. **200**, (1999).
[25] Z. Q. Jin and J. P. Liu, J. Phys. D **39**, R227 (2006).
[26] R. Alben, J. J. Becker, and M. C. Chi, J. Appl. Phys. **49** 1653 (1978).
[27] G. Herzer, Acta Materialia **61**, 718 (2013).
[28] P. Ripka, Sensors and Actuators A **37-38**, 417 (1993).